

Interpretable Stein Goodness-of-fit Tests on Riemannian Manifolds

Wenkai Xu¹ Takeru Matsuda²

¹Gatsby Computational Neuroscience Unit

²Statistical Mathematics Unit, RIKEN Center for Brain Science

Abstract

In many applications, we encounter data on Riemannian manifolds such as torus and rotation groups. Standard statistical procedures for multivariate data are not applicable to such data. In this study, we develop goodness-of-fit testing and interpretable model criticism methods for general distributions on Riemannian manifolds, including those with an intractable normalization constant. The proposed methods are based on extensions of kernel Stein discrepancy, which are derived from Stein operators on Riemannian manifolds. We discuss the connections between the proposed tests with existing ones and provide a theoretical analysis of their asymptotic Bahadur efficiency. Simulation results and real data applications show the validity of the proposed methods.

1 Introduction

In many scientific and machine learning applications, data appear in the domains described by Riemannian manifolds. For example, structures of proteins and molecules are described by a pair of angular variables, which is identified with a point on the torus [Singh et al., 2002]. In computer vision, the orientation of a camera is represented by a 3×3 rotation matrix, which gives rise to data on the rotation group [Song et al., 2009]. Other examples include the orbit of a comet [Jupp et al., 1979] and the vectorcardiogram data [Downs, 1972]. In addition, shape analysis [Dryden and Mardia, 2016] and compositional data analysis [Pawlowsky-Glahn and Buccianti, 2011] also deal with complex data defined on Riemannian manifolds. Recently, [Klein et al., 2020] developed a graphical model on torus to analyze phase coupling between neuronal activities. Since the usual statistical procedures for Euclidean data are not applicable, many studies have developed statistical models and methods tailored for data on Riemannian manifolds [Chikuse, 2012, Mardia and Jupp, 1999, Ley and Verdebout, 2017].

Statistical models on Riemannian manifolds are often given in the form of unnormalized densities with a computationally intractable normalization constant.

For example, the Fisher distribution on the rotation group [Chikuse, 2012, Sei et al., 2013] is defined by

$$p(X | \Theta) \propto \exp(\text{tr}(\Theta^\top X)), \quad (1)$$

and its normalization constant is not given in closed form. Statistical inference with such models can become computationally intensive due to the intractable normalization constant. Thus, statistical methods on Riemannian manifolds that do not require computation of the normalization constant have been developed for several tasks such as parameter estimation [Mardia et al., 2016] and sampling [Girolami et al., 2009, Ma et al., 2015]. However, goodness-of-fit testing or model criticism procedures for general distributions on Riemannian manifolds is not established, to the best of our knowledge.

Kernel Stein discrepancy (KSD) [Gorham and Mackey, 2015, Ley et al., 2017] is a discrepancy measure between distributions based on Stein’s method [Barbour and Chen, 2005, Chen et al., 2010] and reproducing kernel Hilbert space (RKHS) theory [Berlinet and Thomas, 2004]. KSD provides a general procedure for goodness-of-fit testing that does not require computation of the normalization constant, and it has shown state-of-the-art performance in various scenarios including Euclidean data [Chwialkowski et al., 2016, Liu et al., 2016], discrete data [Yang et al., 2018], point processes [Yang et al., 2019], censored data [Fernandez et al., 2020] and directional data [Xu and Matsuda, 2020]. In addition, by using the technique of optimizing test power [Gretton et al., 2012, Sutherland et al., 2016], KSD-based testing procedures also enable extraction of distributional features to perform model criticism [Jitkrittum et al., 2017, Jitkrittum et al., 2018, Kanagawa et al., 2019, Jitkrittum et al., 2020]. We note that Stein’s method has recently been extended to Riemannian manifolds and applied to numerical integration [Barp et al., 2018] and Bayesian inference [Liu and Zhu, 2018].

In this paper, we develop goodness-of-fit testing and interpretable model criticism methods for general distributions on Riemannian manifolds. After briefly reviewing background topics, we first introduce several types of Stein operators on Riemannian manifolds by using Stokes’ theorem. Then, we define manifold kernel Stein discrepancies (mKSD) based on them and propose goodness-of-fit testing procedures, which do not require computation of the normalization constant. We also develop mKSD-based interpretable model criticism procedures. Theoretical comparisons of test performance in terms of Bahadur efficiency are provided, and simulation results validate the claims. Finally, we provide real data applications to demonstrate the usefulness of the proposed methods.

2 Background

2.1 Distributions on Riemannian Manifolds

In this paper, we focus on distributions on a smooth Riemannian manifold (\mathcal{M}, g) , where g is a Riemannian metric on \mathcal{M}^1 . See [Lee, 2018] for details on Riemannian geometry. Here, we give several examples that will be used in experiments. Note that we define the probability density of each distribution by its Radon–Nikodym derivative with respect to the volume element of (\mathcal{M}, g) .

Torus Bivariate circular data $(x_1, x_2) \in [0, 2\pi)^2$ can be viewed as data on the torus $\mathcal{S}_1 \times \mathcal{S}_1$, where we identify $(\cos x, \sin x) \in \mathcal{S}_1$ with $x \in [0, 2\pi)$. To describe dependence between circular variables, [Singh et al., 2002] proposed the bivariate von-Mises distribution:

$$p(x_1, x_2 \mid \xi) \propto \exp(\kappa_1 \cos(x_1 - \mu_1) + \kappa_2 \cos(x_2 - \mu_2) + \lambda_{12} \sin(x_1 - \mu_1) \sin(x_2 - \mu_2)), \quad (2)$$

where $\xi = (\kappa_1, \kappa_2, \mu_1, \mu_2, \lambda_{12})$, $\kappa_1 \geq 0$, $\kappa_2 \geq 0$, $0 \leq \mu_1 < 2\pi$ and $0 \leq \mu_2 < 2\pi$. Its normalization constant is not represented in closed form. We will apply this model to wind direction data in Section 8.

Rotation group The rotation group $\text{SO}(m)$ is defined as

$$\text{SO}(m) = \{X \in \mathbb{R}^{m \times m} \mid X^\top X = I_m, \det X = 1\},$$

where I_m is the m -dimensional identity matrix. The Fisher distribution [Chikuse, 2012, Sei et al., 2013] on $\text{SO}(m)$ is defined as

$$p(X \mid \Theta) \propto \exp(\text{tr}(\Theta^\top X)),$$

for which the normalization constant is not given in closed form. We will apply this model to vectorcardiogram data in Section 8.

The goodness-of-fit testing for general distributions on Riemannian manifolds is not established, to the best of our knowledge. For tests of uniformity, several methods have been proposed such as the Sobolev test [Chikuse and Jupp, 2004, Giné, 1975, Jupp et al., 2008]. However, they are not readily applicable to general distributions. Although there are a few methods applicable to general distributions [Jupp et al., 2005, Jupp and Kume, 2018], they require computation of the normalization constant, which is often computationally intensive. In addition, existing testing procedures cannot be applied to perform interpretable model criticism [Jitkrittum et al., 2016, Kim et al., 2016, Lloyd and Ghahramani, 2015], which would provide an intuitive clarification of the discrepancy between the model and data.

¹In this paper, \mathcal{M} may have non-empty boundary $\partial\mathcal{M}$.

2.2 Kernel Stein Discrepancy on \mathbb{R}^d

Here, we briefly review the goodness-of-fit testing with kernel Stein discrepancy on \mathbb{R}^d . See [Chwialkowski et al., 2016, Liu et al., 2016] for more detail.

Let q be a smooth probability density on \mathbb{R}^d . For a smooth function $\mathbf{f} = (f_1, \dots, f_d) : \mathbb{R}^d \rightarrow \mathbb{R}^d$, the Stein operator \mathcal{T}_q is defined by

$$\mathcal{T}_q \mathbf{f}(x) = \sum_{i=1}^d \left(f_i(x) \frac{\partial}{\partial x^i} \log q(x) + \frac{\partial}{\partial x^i} f_i(x) \right). \quad (3)$$

From integration by parts on \mathbb{R}^d , we obtain the equality, i.e. the Stein's identity $\mathbb{E}_q[\mathcal{T}_q \mathbf{f}] = 0$, under mild regularity conditions. Since Stein operator \mathcal{T}_q depends on the density q only through the derivatives of $\log q$, it does not involve the normalization constant of q , which is a useful property for dealing with unnormalized models [Hyvärinen, 2005].

Let \mathcal{H} be a reproducing kernel Hilbert space (RKHS) on \mathbb{R}^d and \mathcal{H}^d be its product. By using Stein operator, kernel Stein discrepancy (KSD) [Gorham and Mackey, 2015, Ley et al., 2017] between two densities p and q is defined as

$$\text{KSD}(p||q) = \sup_{\|\mathbf{f}\|_{\mathcal{H}^d} \leq 1} \mathbb{E}_p[\mathcal{T}_q \mathbf{f}].$$

It is shown that $\text{KSD}(p||q) \geq 0$ and $\text{KSD}(p||q) = 0$ if and only if $p = q$ under mild regularity conditions [Chwialkowski et al., 2016]. Thus, KSD is a proper discrepancy measure between densities. After some calculation, $\text{KSD}(p||q)$ is rewritten as

$$\text{KSD}^2(p||q) = \mathbb{E}_{x, \tilde{x} \sim p}[h_q(x, \tilde{x})], \quad (4)$$

where h_q does not involve p .

Given samples x_1, \dots, x_n from *unknown* density p on \mathbb{R}^d , an empirical estimate of $\text{KSD}^2(p||q)$ can be obtained by using Eq.(4) in the form of U-statistics, and this estimate is used to test the hypothesis $H_0 : p = q$, where the critical value is determined by bootstrap. In this way, a general method of non-parametric goodness-of-fit test on \mathbb{R}^d is obtained, which does not require computation of the normalization constant.

3 Stein Operators on \mathcal{M}

In this section, we introduce several types of Stein operators for distributions on Riemannian manifolds by using Stokes' theorem. The operators are categorized via the order of differentials of the input functions².

²Note that this should be distinguished from the differentials of the (unnormalized) density functions.

3.1 Differential Forms and Stokes' Theorem

To derive Stein operators on Riemannian manifolds, we need to use differential forms and Stokes' theorem. Here, we briefly introduce these concepts. For more detailed and rigorous treatments, see [Flanders, 1963, Lee, 2018, Spivak, 2018].

Let \mathcal{M} be a smooth d -dimensional Riemannian manifold and take its local coordinate system x^1, \dots, x^d . We introduce symbols dx^1, \dots, dx^d and an associative and anti-symmetric operation \wedge between them called the wedge product: $dx^i \wedge dx^j = -dx^j \wedge dx^i$. Note that $dx^i \wedge dx^i = 0$. Then, a p -form ω on M ($0 \leq p \leq d$) is defined as

$$\omega = \sum_{i_1 \dots i_p} f_{i_1 \dots i_p} dx^{i_1} \wedge \dots \wedge dx^{i_p},$$

where the sum is taken over all p -tuples $\{i_1, \dots, i_p\} \subset \{1, \dots, d\}$ and each $f_{i_1 \dots i_p}$ is a smooth function on \mathcal{M} . The exterior derivative $d\omega$ of ω is defined as the $(p+1)$ -form given by

$$d\omega = \sum_{i_1 \dots i_p} \sum_{i=1}^d \frac{\partial f_{i_1 \dots i_p}}{\partial x^i} dx^i \wedge dx^{i_1} \wedge \dots \wedge dx^{i_p}.$$

For another coordinate system y^1, \dots, y^d on \mathcal{M} , the differential form is transformed by

$$dy^j = \sum_{i=1}^d \frac{\partial y^j}{\partial x^i} dx^i.$$

The volume element is defined as the d -form given by

$$(\det g)^{1/2} dx^1 \wedge \dots \wedge dx^d,$$

where $g = g(x^1, \dots, x^d)$ is the $d \times d$ matrix of the Riemannian metric with respect to x^1, \dots, x^d .

The integration of a d -form on a d -dimensional manifold is naturally defined like the usual integration on \mathbb{R}^d and invariant with respect to the coordinate selection. Correspondingly, the integration by parts formula on \mathbb{R}^d is generalized in the form of Stokes' theorem.

Proposition 1 (Stokes' theorem). *Let $\partial\mathcal{M}$ be the boundary of \mathcal{M} and ω be a $(d-1)$ -form on \mathcal{M} . Then,*

$$\int_{\mathcal{M}} d\omega = \int_{\partial\mathcal{M}} \omega.$$

Corollary 1. *If $\partial\mathcal{M}$ is empty, then $\int_{\mathcal{M}} d\omega = 0$ for any $(d-1)$ -form ω on \mathcal{M} .*

Coordinate choice In the following, to facilitate the derivation as well as computation of Stein operators, we assume that there exists a coordinate system $\theta^1, \dots, \theta^d$ on \mathcal{M} that covers \mathcal{M} almost everywhere. For example, spherical coordinates for the hyperspheres and torus, generalized Euler angles [Chikuse, 2012, Section 2.5.1] for the rotation groups, and Givens rotations [Pourzanjani et al., 2017] for the Stiefel manifolds satisfy this assumption.

3.2 First Order Stein Operator

For a smooth probability density q on \mathcal{M} and a smooth function $\mathbf{f} = (f^1, \dots, f^d) : \mathcal{M} \rightarrow \mathbb{R}^d$, define a function $\mathcal{A}_q^{(1)}\mathbf{f} : \mathcal{M} \rightarrow \mathbb{R}$ by

$$\mathcal{A}_q^{(1)}\mathbf{f} = \sum_{i=1}^d \left(\frac{\partial f^i}{\partial \theta^i} + f^i \frac{\partial}{\partial \theta^i} \log(qJ) \right), \quad (5)$$

where $J = (\det g)^{1/2}$ is the volume element. We refer to $\mathcal{A}_q^{(1)}$ as the first order Stein operator. Note that [Xu and Matsuda, 2020] utilized this operator for goodness-of-fit testing on hyperspheres.

Theorem 1. *If $\partial\mathcal{M}$ is empty or f^1, \dots, f^d vanish on $\partial\mathcal{M}$, then*

$$\mathbb{E}_q[\mathcal{A}_q^{(1)}\mathbf{f}] = 0.$$

If \mathcal{M} is a closed manifold such as torus and rotation group, it does not have boundary by definition and thus the assumption of Theorem 1 holds. If the boundary of \mathcal{M} is non-empty, a discussion relevant to the assumption of Theorem 1 can be found in [Liu and Kanamori, 2019], which studies density estimation on truncated domains. Note that the assumption of Theorem 1 is similar to Assumption 4 in [Barp et al., 2018].

3.3 Second Order Stein Operator

In the context of numerical integration on Riemannian manifolds, [Barp et al., 2018] introduced a different type of Stein operator $\mathcal{A}_q^{(2)}$, which we call the second order Stein operator. Specifically, for a smooth probability density q on \mathcal{M} and a smooth function $\tilde{f} : \mathcal{M} \rightarrow \mathbb{R}$, define $\mathcal{A}_q^{(2)}\tilde{f} : \mathcal{M} \rightarrow \mathbb{R}$ by

$$\mathcal{A}_q^{(2)}\tilde{f} = \sum_{ij} \left(g^{ij} \frac{\partial^2 \tilde{f}}{\partial \theta^i \partial \theta^j} + g^{ij} \frac{\partial \tilde{f}}{\partial \theta^j} \frac{\partial \log qJ}{\partial \theta^i} \right) \quad (6)$$

where we denote the inverse matrix of (g_{ij}) by (g^{ij}) following the convention of Riemannian geometry.

Proposition 2 (Proposition 1 of [Barp et al., 2018]). *If $\partial\mathcal{M}$ is empty or \tilde{f} vanishes on $\partial\mathcal{M}$, then*

$$\mathbb{E}_q[\mathcal{A}_q^{(2)}\tilde{f}] = 0.$$

Theorem 2 follows from Theorem 1, because the second order Stein operator in Eq.(6) can be viewed as a special case of the first order Stein operator in Eq.(5) with

$$f^i = \sum_j g^{ij} \frac{\partial \tilde{f}}{\partial \theta^j}. \quad (7)$$

Similar form of the second order Stein operator in Eq.(6) has been studied in [Liu and Zhu, 2018] for Bayesian inference. On the other hand, [Le et al., 2020] arrives at a similar second order Stein operator on Riemannian manifolds via Feller diffusion process in the context of density approximation.

3.4 Zeroth Order Stein Operator

For a smooth probability density q on \mathcal{M} and a function $h : \mathcal{M} \rightarrow \mathbb{R}$, define a function $\mathcal{A}_q^{(0)}h : \mathcal{M} \rightarrow \mathbb{R}$ by

$$\mathcal{A}_q^{(0)}h = h - \mathbb{E}_q[h],$$

which clearly satisfies $\mathbb{E}_q[\mathcal{A}_q^{(0)}h] = 0$. Since $\mathcal{A}_q^{(0)}$ does not involve any differentials, we call it the zeroth order Stein operator. Compared to the first and second order Stein operators, this operator requires the normalization constant of q , which is often computationally intractable for Riemannian manifolds. We will show later that this operator corresponds to the maximum mean discrepancy [Gretton et al., 2007].

4 Goodness-of-fit Tests on \mathcal{M}

In this section, we propose goodness-of-fit testing procedures for distributions on Riemannian manifolds based on Stein operators in the previous section.

4.1 Manifold Kernel Stein Discrepancies

By using Stein operators introduced in the previous section, we extend kernel Stein discrepancy to distributions on Riemannian manifolds.

Let \mathcal{H} be a RKHS on \mathcal{M} with reproducing kernel k and \mathcal{H}^d be its product. We define the manifold kernel Stein discrepancies (mKSD) of the first, second and zeroth

order by

$$\begin{aligned}\text{mKSD}^{(1)}(p\|q) &= \sup_{\|\mathbf{f}\|_{\mathcal{H}^d} \leq 1} \mathbb{E}_p[\mathcal{A}_q^{(1)}\mathbf{f}], \\ \text{mKSD}^{(2)}(p\|q) &= \sup_{\|\tilde{f}\|_{\mathcal{H}} \leq 1} \mathbb{E}_p[\mathcal{A}_q^{(2)}\tilde{f}], \\ \text{mKSD}^{(0)}(p\|q) &= \sup_{\|h\|_{\mathcal{H}} \leq 1} \mathbb{E}_p[\mathcal{A}_q^{(0)}h],\end{aligned}$$

respectively. We also define the Stein kernels of first, second and zeroth order by

$$\begin{aligned}h_q^{(1)}(x, \tilde{x}) &= \left\langle \mathcal{A}_q^{(1)}k(x, \cdot), \mathcal{A}_q^{(1)}k(\tilde{x}, \cdot) \right\rangle_{\mathcal{H}^d}, \\ h_q^{(2)}(x, \tilde{x}) &= \left\langle \mathcal{A}_q^{(2)}k(x, \cdot), \mathcal{A}_q^{(2)}k(\tilde{x}, \cdot) \right\rangle_{\mathcal{H}}, \\ h_q^{(0)}(x, \tilde{x}) &= \left\langle \mathcal{A}_q^{(0)}k(x, \cdot), \mathcal{A}_q^{(0)}k(\tilde{x}, \cdot) \right\rangle_{\mathcal{H}},\end{aligned}$$

respectively. Then, by algebraic manipulation, we obtain the following.

Theorem 2. *If p and q are smooth densities on \mathcal{M} and the reproducing kernel k of \mathcal{H} is smooth, then*

$$\text{mKSD}^{(c)}(p\|q)^2 = \mathbb{E}_{x, \tilde{x}}[h_q^{(c)}(x, \tilde{x})] \quad (8)$$

for $c = 0, 1, 2$, where $x, \tilde{x} \sim p$ are independent.

From Theorem 2, we can estimate mKSD by using samples from p . This is an important property in goodness-of-fit testing.

The following theorem shows that mKSD is a proper discrepancy measure between distributions on Riemannian manifolds. The proof is given in supplementary material. Let $L(x) = (L_1(x), \dots, L_d)^\top \in \mathbb{R}^d$ with

$$L_i(x) = \frac{\partial}{\partial \theta^i} \log \frac{q(x)}{p(x)}.$$

Theorem 3. *Let p and q be smooth densities on \mathcal{M} . Assume: 1) The kernel k vanishes at $\partial\mathcal{M}$ and is compact universal in the sense of [Carmeli et al., 2010, Definition 2 (ii)]; 2) $\mathbb{E}_{x, \tilde{x} \sim p}[h_q^{(c)}(x, \tilde{x})^2] < \infty$, for $c = 0, 1, 2$; 3) $\mathbb{E}_p\|L(x)\|^2 < \infty$. Then, $\text{mKSD}^{(c)}(p\|q) \geq 0$ and $\text{mKSD}^{(c)}(p\|q) = 0$ if and only if $p = q$.*

Note that different mKSD uses different RKHS as the space of test functions. With the d -dimensional vector valued RKHS \mathcal{H}^d , $\text{mKSD}^{(1)}$ takes the supremum over a larger class of functions than $\text{mKSD}^{(2)}$, capturing richer distribution features. Theoretical analysis in testing context will be presented in Section 6.

Equivalence of mKSD⁽⁰⁾ and MMD For a RKHS \mathcal{H} , the maximum mean discrepancy (MMD) [Gretton et al., 2007] between p and q is defined by

$$\text{MMD}(p\|q)^2 = \|\mu_p - \mu_q\|_{\mathcal{H}}^2,$$

where μ_p, μ_q are the kernel mean embeddings [Muandet et al., 2017] of p and q , respectively. The following theorem shows that mKSD⁽⁰⁾ is equivalent to MMD.

Theorem 4.

$$\text{mKSD}^{(0)}(p\|q) = \text{MMD}(p\|q).$$

Proof. By definition, we have

$$\begin{aligned} \text{mKSD}^{(0)}(p\|q) &= \sup_{\|h\|_{\mathcal{H}} \leq 1} \mathbb{E}_p[\mathcal{A}_q^{(0)}h] \\ &= \sup_{\|h\|_{\mathcal{H}} \leq 1} (\mathbb{E}_p[h] - \mathbb{E}_q[h]). \end{aligned}$$

Hence, taking the supreme in closed form via reproducing property, we obtain

$$\text{mKSD}^{(0)}(p\|q)^2 = \|\mu_p - \mu_q\|_{\mathcal{H}}^2 = \text{MMD}(p\|q)^2.$$

□

4.2 Goodness-of-fit Testing with mKSDs

Here, we present procedures for testing $H_0 : p = q$ with significance level α based on samples $x_1, \dots, x_n \sim p$.

From Theorem 2, an unbiased estimate of mKSD can be obtained in the form of U-statistics [Lee, 1990]:

$$\text{mKSD}_u^{(c)}(p\|q)^2 = \frac{1}{n(n-1)} \sum_{i \neq j} h_q^{(c)}(x_i, x_j). \quad (9)$$

Its asymptotic distribution is obtained via U-statistics theory [Lee, 1990, Van der Vaart, 2000] as follows. We denote the convergence in distribution by \xrightarrow{d} .

Theorem 5. For $c = 0, 1, 2$, the following statements hold.

1. Under $H_0 : p = q$,

$$n \cdot \text{mKSD}_u^{(c)}(p\|q)^2 \xrightarrow{d} \sum_{j=1}^{\infty} w_j^{(c)} (Z_j^2 - 1), \quad (10)$$

where Z_j are i.i.d. standard Gaussian random variables and $w_j^{(c)}$ are the eigenvalues of the Stein kernel $h_q^{(c)}(x, \tilde{x})$ under $p(\tilde{x})$:

$$\int h_q^{(c)}(x, \tilde{x}) \phi_j(\tilde{x}) p(\tilde{x}) d\tilde{x} = w_j^{(c)} \phi_j(x), \quad (11)$$

where $\phi_j(x) \neq 0$ is the non-trivial eigen-function.

2. Under $H_1 : p \neq q$,

$$\sqrt{n} \cdot \left(\text{mKSD}_u^{(c)}(p||q)^2 - \text{mKSD}^{(c)}(p||q)^2 \right) \xrightarrow{d} \mathcal{N}(0, \sigma_c^2),$$

where $\sigma_c^2 = \text{Var}_{x \sim p}[\mathbb{E}_{\tilde{x} \sim p}[h_q^{(c)}(x, \tilde{x})]] > 0$.

Based on Theorem 5, we propose two procedures for goodness-of-fit testing.

Spectrum Test We can also directly approximate the null distribution in Eq.(10) by using the eigenvalues of the Stein kernel matrix [Gretton et al., 2009, Theorem 1]. Specifically, let $M^{(c)}$ be the $n \times n$ Stein kernel matrix defined by $(M^{(c)})_{ij} = h_q^{(c)}(x_i, x_j)$ and $\tilde{w}_1^{(c)}, \dots, \tilde{w}_n^{(c)}$ be its eigenvalues. Then, we define the bootstrap samples by

$$S_t = \frac{1}{n} \sum_{j=1}^n \tilde{w}_j^{(c)} (Z_{j,t}^2 - 1), \quad (12)$$

where each $Z_{j,t}$ is the standard Gaussian variable.

Wild-bootstrap Test We employ the wild-bootstrap test with the V-statistics [Chwialkowski et al., 2014]. The test statistic is given by

$$\text{mKSD}_v^{(c)}(p||q)^2 = \frac{1}{n^2} \sum_{i,j} h_q^{(c)}(x_i, x_j). \quad (13)$$

To approximate its null distribution, we define the wild-bootstrap samples by

$$S_t = \frac{1}{n^2} \sum_{i,j} W_{i,t} W_{j,t} h_q^{(c)}(x_i, x_j), \quad (14)$$

where each $W_{i,t} \in \{-1, 1\}$ is the Rademacher variable of zero mean and unit variance.

The testing procedure is outlined in Algorithm 1. We adopt this algorithm in the following experiments due to its computational efficiency.

Kernel choice The performance of kernel-based testing is sensitive to the choice of kernel parameters. We choose the kernel parameters by maximizing an approximation of the test power following [Gretton et al., 2012, Jitkrittum et al., 2016, Sutherland et al., 2016]. From Theorem 5,

$$D := \sqrt{n} \frac{\text{mKSD}_u^2(p||q) - \text{mKSD}^2(p||q)}{\sigma_c} \xrightarrow{d} \mathcal{N}(0, 1)$$

under the alternative $H_1 : p \neq q$. Thus, for sufficiently large n , the test power is approximated as $\Pr_{H_1}(n \cdot \text{mKSD}_u^{(c)}(p||q)^2 > r) \approx \Phi\left(\sqrt{n} \frac{\text{mKSD}^{(c)}(p||q)^2}{\sigma_c}\right)$ [Sutherland et al., 2016]. Thus, we choose the kernel parameters by maximizing an estimate of $\text{mKSD}^2(p||q)/\sigma_c$ [Jitkrittum et al., 2017].

Algorithm 1 mKSD test via wild-bootstrap

Input:

samples $x_1, \dots, x_n \sim p$, null density q
kernel function k , test size α
bootstrap sample size B

Objective:

Test $H_0 : p = q$ versus $H_1 : p \neq q$.

Test procedure:

- 1: Compute the statistic $\text{mKSD}_v^{(c)}(p||q)^2$, Eq.(9).
- 2: **for** $t = 1 : B$ **do**
- 3: Sample Rademacher variables $W_{1,t}, \dots, W_{n,t}$.
- 4: Compute S_t by Eq.(14).
- 5: **end for**
- 6: Determine the $(1 - \alpha)$ -quantile $\gamma_{1-\alpha}$ of S_1, \dots, S_B .

Output:

Reject H_0 if $\text{mKSD}_v^{(c)}(p||q)^2 > \gamma_{1-\alpha}$; otherwise do not reject H_0 .

5 Model Criticism on \mathcal{M}

Now, we propose mKSD-based model criticism procedures for distributions on Riemannian manifolds. When the proposed model does not fit the observed data well, understanding which part of the model misfit the data is of practical interest. The model criticism study can be helpful to better understand the representative prototype [Kim et al., 2016], to criticize prior assumptions in Bayesian settings [Lloyd and Ghahramani, 2015] or to help better training of generative models [Sutherland et al., 2016]. With kernel-based non-parametric testing, distributional features can be extracted in the form of *test locations* to represent areas that “best distinguish” distributions. The locations where two sample distributions differ the most via MMD are studied in [Jitkrittum et al., 2016] and the most “mis-specified” locations between samples and models via KSD are studied in [Jitkrittum et al., 2017]. Recently, [Seth et al., 2019] studied the model criticism via latent space, which may intrinsically correspond to Riemannian manifold structures. Such setting can be an interesting application of our development.

Let $\mathbf{s}_p(\cdot) = \mathbb{E}_{\tilde{x} \sim p}[\mathcal{A}_q^{(1)}k(\tilde{x}, \cdot)] \in \mathcal{H}^d$. We define the manifold Finite Set Stein Discrepancy (mFSSD) adapted from [Jitkrittum et al., 2017] by

$$\text{mFSSD}^2 = \frac{1}{dJ} \sum_{i=1}^d \sum_{j=1}^J (\mathbf{s}_p(\mathbf{v}_j))_i^2, \quad (15)$$

which can be computed in linear time of sample size n . Stein identity of $\mathbf{s}_p(\cdot)$ ensures $\text{mFSSD}^2 = 0$ under H_0 with probability one [Jitkrittum et al., 2017, Theorem 1]. To perform model criticism, we extract some test locations that give a higher detection

rate (i.e., test power) than others. We choose the test locations $V = \{\mathbf{v}_j\}_{j=1}^J$ by maximizing the approximate test power:

$$V = \arg \max_{\mathbf{v}} \frac{\text{mFSSD}^2}{\tilde{\sigma}_{H_1}}, \quad (16)$$

where $\tilde{\sigma}_{H_1}$ is the variance of mFSSD^2 under H_1 . More details are shown in Proposition 3 and 4 in the supplementary material.

6 Comparison between mKSD Tests

Bahadur efficiency From Theorem 5, mKSD tests are consistent against all alternatives. Thus, to understand which mKSD test is more powerful than others, we investigated their *Bahadur efficiency* [Bahadur et al., 1960], which quantify how fast the p-value goes to zero under alternatives. Here, to focus on the effect of the choice of Stein operator on test performance, we briefly present results for testing of uniformity on the circle \mathcal{S}^1 under the von-Mises distribution. See supplementary material for more details. The technique of the proof is adapted from [Jitkrittum et al., 2017].

Theorem 6. (*Scaling shift in von-Mises distribution*) Let $x \in \mathcal{S}^1$, $q(x) \propto 1$ and $p(x) \propto \exp(\kappa u^\top x)$. Choose the von-Mises kernel of the form $k(x, x') = \exp(x^\top x')$. Denote the approximate Bahadur efficiency between mKSD with first and second order Stein operators as

$$E_{1,2}(\kappa) := \frac{c^{(\text{mKSD}^{(1)})}(\kappa)}{c^{(\text{mKSD}^{(2)})}(\kappa)},$$

where $\kappa > 0$. Then $E_{1,2}(\kappa) > 1$.

Adapting [Jitkrittum et al., 2017, Theorem 5], it suffices to show $\text{mKSD}^{(1)}(p||q) \geq \text{mKSD}^{(2)}(p||q)$ and

$$\mathbb{E}_{x, \tilde{x} \sim q}[h_q^{(2)}(x, \tilde{x})^2] > \mathbb{E}_{x, \tilde{x} \sim q}[h_q^{(1)}(x, \tilde{x})^2] > 0.$$

See supplementary material for details.

We provide additional discussion on the relative test efficiencies with $\text{mKSD}^{(0)}$ in the supplementary material. In general, since we cannot compute \mathbb{E}_p in closed form, especially with unnormalized density, we need to perform the test with samples drawn from the null, where sampling error makes the $\text{mKSD}^{(0)}$ test less efficient in overall [Jitkrittum et al., 2017, Yang et al., 2019, Xu and Matsuda, 2020].

Computational efficiency Since the Stein kernels $h_q^{(1)}$ and $h_q^{(2)}$ depend on q only through the derivative of $\log q$, mKSD tests with the first and second order Stein operators do not require computation of the normalization constant of q . This is a

major computational advantage over existing goodness-of-fit tests on Riemannian manifolds. While the computational cost of $\text{mKSD}_u^{(1)}$ is $O(n^2d)$, that of $\text{mKSD}^{(2)}$ is $O(n^2d^3)$ due to the computation of the metric tensor.

On the other hand, mKSD test of zeroth order is equivalent to testing whether two sets of samples are from the same distribution by using MMD [Gretton et al., 2007]. Namely, to test whether x_1, \dots, x_n is from density q , we draw samples y_1, \dots, y_m from q and determine whether x_1, \dots, x_n and y_1, \dots, y_m are from the same distribution. This procedure requires to sample from the null distribution q on Riemannian manifolds, which is computationally intensive in general. Note that the results in Theorem 5 with $c = 0$ replicate the asymptotic results for MMD [Gretton et al., 2007].

Choosing mKSD tests Overall, $\text{mKSD}^{(1)}$ has its advantage in terms of having a large space of test functions with both asymptotic test efficiency and computational efficiency so that it is recommended to use when available. $\text{mKSD}^{(2)}$ can be slightly easier to compute and parameterize in particular scenarios, although it may sacrifice test power and computational efficiency. $\text{mKSD}^{(0)}$, or namely MMD test, is also applicable when it is possible to sample from the given unnormalized density model on Riemannian manifolds.

7 Simulation Results

In this section, we show the validity of the proposed mKSD tests by simulation on the rotation group $\text{SO}(3)$. We use the Euler angle [Chikuse, 2012] as the coordinate system. The bootstrap sample size is set to $B = 1000$. The significance level is set to $\alpha = 0.01$. For the $\text{mKSD}^{(0)}$ test (MMD two-sample test), the number of samples from the null is set to be equal to the sample size n . We used the kernel $k(X, Y) = \exp(\eta \cdot \text{tr}(X^\top Y))$, where the parameter η was chosen by optimizing the approximate test power. The exponential-trace kernel $k(X, Y) = \exp(\eta \cdot \text{tr}(X^\top Y))$ for the rotation group is compact universal. To see this, we rewrite the kernel in the form analogous to the Gaussian kernel: $k(X, Y) = \exp(\eta \cdot \text{tr}(X^\top Y)) = C \cdot \exp(-\frac{1}{2}\eta \cdot \|X - Y\|_F^2)$, where C is a constant that only depends on d , the dimension of the matrices $X, Y \in \text{SO}(d)$ and we know that $\text{tr}(X^\top X) = \text{tr}(I_d) = d$ for all $X \in \text{SO}(d)$. Then, since the Gaussian kernel is universal [Sriperumbudur et al., 2011] and the rotation group $\text{SO}(d)$ is a compact subset of the space of $d \times d$ matrices, the exponential-trace kernel is also compact-universal from Corollary 3 of [Carmeli et al., 2010].

7.1 Uniform distribution

First, we consider testing of uniformity on $\text{SO}(3)$ and compare the performance of the mKSD tests with the Sobolev test [Jupp et al., 2005]. We generated samples

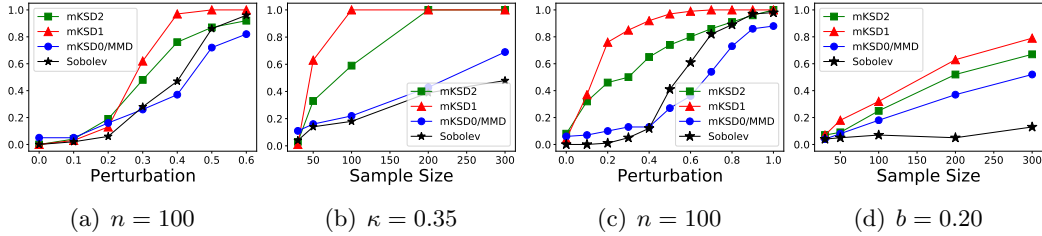


Figure 1: Rejection rates at $\alpha = 0.01$: a)-b) for uniform density; c)-d) for Fisher distribution on $SO(3)$

from the exponential trace distribution $p(X | \kappa) \propto \exp(\kappa \cdot \text{tr}(X))$ by the rejection sampling [Hoff, 2009]. The uniform distribution corresponds to $\kappa = 0$.

Figure 1 (a) plots the rejection rates with respect to κ for $n = 100$. When $\kappa = 0$, the type-I errors of all tests are well controlled to the significance level $\alpha = 0.01$. The power of all tests increases with increasing κ and converges to one. Figure 1 (b) plots the rejection rates with respect to n for $\kappa = 0.35$. The power of all tests increases with n and converges to one. When the model becomes increasingly different from the null, the mKSD1 is more sensitive to distinguish the difference, with higher power than others.

7.2 Fisher distribution

Next, we consider the Fisher distribution (or matrix-Langevin distribution) $p(X | F) \propto \exp(\text{tr}(F^T X))$ [Chikuse, 2003, Sei et al., 2013]. We generated data from $p(X | F_0)$ and applied mKSD tests on the null $p(X | F_b)$, where

$$F_b = \begin{pmatrix} 1 & b & 0 \\ b & 1 & 0 \\ 0 & 0 & 1 \end{pmatrix}.$$

We compare the mKSD tests with the extended Sobolev test [Jupp et al., 2005], in which we compute the normalization constant by Monte Carlo.

Figure 1 (c) plots the rejection rates with respect to b for $n = 100$. Figure 1 (d) plots the rejection rates with respect to n for $b = 0.2$. From the plot, we see that all tests achieves the correct test level under the null. When the model becomes increasingly different from the null, the mKSD1 is more sensitive to distinguish the difference, with higher power than others. MMD test has lower power than mKSD1 and mKSD2 due to inefficiency from sampling. While the Sobolev test is useful when the null and the alternative are very different, it is not powerful for harder problems where the alternative perturbed very little from the null.

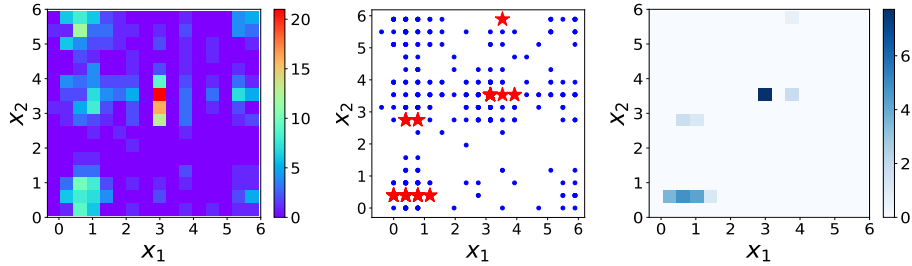


Figure 2: Wind direction data. Left: 2D histogram for wind directions; colorbar shows the counts of data points in each square. Mid: the 10 optimized locations (in red star), without repetition. Right: the objective value in Eq.(16), $\frac{mFSSD^2}{\sigma_{H_1}}$, on the specified data location of test (i.e. setting $J=1$); the higher the darker.

8 Real Data Applications

Finally, we apply the mKSD tests to two real data problems.

8.1 Vectorcardiogram data

As a real dataset on the rotation group $SO(3)$, we use the vectorcardiogram data studied by [Jupp et al., 2008]. The data summarizes vectorcardiogram from normal children where each data point records 3 perpendicular vectors of directions QRS, PRS and T from Frank system for electrical lead placement. Details of this dataset can be found in [Downs, 1972]. [Jupp et al., 2005] fitted the Fisher distribution $p(X | F) \propto \exp(\text{tr}(F^\top X))$ to 28 data points of children aged between 2 to 10 and obtained the estimate

$$\hat{F} = 5.63 \times \begin{pmatrix} 0.583 & 0.629 & 0.514 \\ 0.660 & -0.736 & 0.151 \\ 0.473 & 0.252 & -0.844 \end{pmatrix}.$$

We use this value as the null model to be tested. Table 1 presents the p-values of each test³. All mKSD tests show strong evidence to reject the fitted model at $\alpha = 0.05$; however, Sobolev test, with p-value=0.126, is not powerful enough to reject the null at the same test level.

Table 1: p-values for vectorcardiogram data.

mKSD1	mKSD2	mKSD0/MMD	Sobolev
0.004	0.000	0.010	0.126

³ $k(X, Y) = \exp(\eta \cdot \text{tr}(X^\top Y))$ is used as in Section 7.

8.2 Wind direction data

As a real data on torus, we consider wind direction in Tokyo on 00:00 (x_1) and 12:00 (x_2) for each day in 2018⁴. Thus, the sample size is $n = 365$. The data were discretized into 16 directions, such as north-northeast. Figure 2 presents a 16×16 histogram of raw data.

We consider goodness-of-fit testing of the bivariate von Mises distribution in Eq.(2) via mKSD⁵. By using noise contrastive estimation [Gutmann and Hyvärinen, 2012], [Uehara et al., 2020] fitted the bivariate von Mises distribution to the wind direction data and obtained the estimate

$$\hat{\xi} = (0.7170, 0.3954, 1.1499, 1.1499, -1.1274).$$

By setting this fitted model to the null model, the p-value by mKSD1 is 0.434, which indicates that the model fits data well.

In addition, we fitted a simpler model with no interactions between x_1 and x_2 , i.e. λ_{12} is set to zero in Eq.(2) so that the model reduces to the product of two von-Mises distribution on each direction. The p-value by mKSD1 is 0.002, which is a strong evidence to reject the null model. In other words, there is a significant interaction between wind direction on 00:00 and 12:00. We then carried out model criticism by mFFSD statistic in Eq.(15) with optimized test location via maximizing approximate test power. Choosing the number of test locations $J = 10$, we plot the optimized locations in Figure 2. It provides information about dependence between wind direction at midnight and noon.

Acknowledgement

TM was supported by JSPS KAKENHI Grant Number 19K20220. WX was supported by Gatsby Charitable Foundation.

References

- [Bahadur et al., 1960] Bahadur, R. R. et al. (1960). Stochastic comparison of tests. *Annals of Mathematical Statistics*, 31(2):276–295.
- [Barbour and Chen, 2005] Barbour, A. D. and Chen, L. H. Y. (2005). *An introduction to Stein’s method*, volume 4. World Scientific.
- [Barp et al., 2018] Barp, A., Oates, C., Porcu, E., and Girolami, M. (2018). A riemannian-stein kernel method. *arXiv preprint arXiv:1810.04946*.

⁴available on Japan Meteorological Agency website

⁵We used the product kernel of the von Mises kernels $k((x_1, x_2), (y_1, y_2)) = \exp(\eta_1 \cos(x_1 - y_1) + \eta_2 \cos(x_2 - y_2))$, where the parameters η_1 and η_2 were chosen by optimizing the approximate test power

- [Berlinet and Thomas, 2004] Berlinet, A. and Thomas, C. (2004). *Reproducing kernel Hilbert spaces in Probability and Statistics*. Kluwer Academic Publishers.
- [Carmeli et al., 2010] Carmeli, C., De Vito, E., Toigo, A., and Umanitá, V. (2010). Vector valued reproducing kernel hilbert spaces and universality. *Analysis and Applications*, 8(01):19–61.
- [Chen et al., 2010] Chen, L. H. Y., Goldstein, L., and Shao, Q. M. (2010). *Normal approximation by Stein’s method*. Springer.
- [Chikuse, 2003] Chikuse, Y. (2003). Concentrated matrix langevin distributions. *Journal of Multivariate Analysis*, 2(85):375–394.
- [Chikuse, 2012] Chikuse, Y. (2012). *Statistics on special manifolds*, volume 174. Springer Science & Business Media.
- [Chikuse and Jupp, 2004] Chikuse, Y. and Jupp, P. E. (2004). A test of uniformity on shape spaces. *Journal of multivariate analysis*, 88(1):163–176.
- [Chwialkowski et al., 2016] Chwialkowski, K., Strathmann, H., and Gretton, A. (2016). A kernel test of goodness of fit. In *International Conference on Machine Learning*, pages 2606–2615.
- [Chwialkowski et al., 2014] Chwialkowski, K. P., Sejdinovic, D., and Gretton, A. (2014). A wild bootstrap for degenerate kernel tests. In *Advances in neural information processing systems*, pages 3608–3616.
- [Downs, 1972] Downs, T. D. (1972). Orientation statistics. *Biometrika*, 59(3):665–676.
- [Dryden and Mardia, 2016] Dryden, I. L. and Mardia, K. V. (2016). *Statistical shape analysis: with applications in R*, volume 995. John Wiley & Sons.
- [Fernandez et al., 2020] Fernandez, T., Rivera, N., Xu, W., and Gretton, A. (2020). Kernelized stein discrepancy tests of goodness-of-fit for time-to-event data. *arXiv preprint arXiv:2008.08397*.
- [Flanders, 1963] Flanders, H. (1963). *Differential Forms with Applications to the Physical Sciences*. Dover.
- [Garreau et al., 2017] Garreau, D., Jitkrittum, W., and Kanagawa, M. (2017). Large sample analysis of the median heuristic. *arXiv preprint arXiv:1707.07269*.
- [Giné, 1975] Giné, E. (1975). Invariant tests for uniformity on compact riemannian manifolds based on sobolev norms. *The Annals of statistics*, pages 1243–1266.
- [Girolami et al., 2009] Girolami, M., Calderhead, B., and Chin, S. A. (2009). Riemannian manifold hamiltonian monte carlo. *arXiv preprint arXiv:0907.1100*.

- [Gleser, 1966] Gleser, L. J. (1966). The comparison of multivariate tests of hypothesis by means of bahadur efficiency. *Sankhyā: The Indian Journal of Statistics, Series A*, pages 157–174.
- [Gorham and Mackey, 2015] Gorham, J. and Mackey, L. (2015). Measuring sample quality with stein’s method. In *Advances in Neural Information Processing Systems*, pages 226–234.
- [Gretton et al., 2007] Gretton, A., Borgwardt, K., Rasch, M., Schölkopf, B., and Smola, A. J. (2007). A kernel method for the two-sample-problem. In *Advances in neural information processing systems*, pages 513–520.
- [Gretton et al., 2009] Gretton, A., Fukumizu, K., Harchaoui, Z., and Sriperumbudur, B. K. (2009). A fast, consistent kernel two-sample test. In *Advances in neural information processing systems*, pages 673–681.
- [Gretton et al., 2012] Gretton, A., Sejdinovic, D., Strathmann, H., Balakrishnan, S., Pontil, M., Fukumizu, K., and Sriperumbudur, B. K. (2012). Optimal kernel choice for large-scale two-sample tests. In *Advances in neural information processing systems*, pages 1205–1213.
- [Gutmann and Hyvärinen, 2012] Gutmann, M. U. and Hyvärinen, A. (2012). Noise-contrastive estimation of unnormalized statistical models, with applications to natural image statistics. *Journal of Machine Learning Research*, 13:307–361.
- [Hoff, 2009] Hoff, P. D. (2009). Simulation of the matrix bingham–von mises–fisher distribution, with applications to multivariate and relational data. *Journal of Computational and Graphical Statistics*, 18(2):438–456.
- [Hyvärinen, 2005] Hyvärinen, A. (2005). Estimation of non-normalized statistical models by score matching. *Journal of Machine Learning Research*, 6(Apr):695–709.
- [Jitkrittum et al., 2018] Jitkrittum, W., Kanagawa, H., Sangkloy, P., Hays, J., Schölkopf, B., and Gretton, A. (2018). Informative features for model comparison. In *Advances in Neural Information Processing Systems*, pages 808–819.
- [Jitkrittum et al., 2020] Jitkrittum, W., Kanagawa, H., and Schölkopf, B. (2020). Testing goodness of fit of conditional density models with kernels. *arXiv preprint arXiv:2002.10271*.
- [Jitkrittum et al., 2016] Jitkrittum, W., Szabó, Z., Chwialkowski, K. P., and Gretton, A. (2016). Interpretable distribution features with maximum testing power. In *Advances in Neural Information Processing Systems*, pages 181–189.
- [Jitkrittum et al., 2017] Jitkrittum, W., Xu, W., Szabó, Z., Fukumizu, K., and Gretton, A. (2017). A linear-time kernel goodness-of-fit test. In *Advances in Neural Information Processing Systems*, pages 262–271.

- [Jupp et al., 2005] Jupp, P. et al. (2005). Sobolev tests of goodness of fit of distributions on compact riemannian manifolds. *The Annals of Statistics*, 33(6):2957–2966.
- [Jupp et al., 2008] Jupp, P. et al. (2008). Data-driven sobolev tests of uniformity on compact riemannian manifolds. *The Annals of Statistics*, 36(3):1246–1260.
- [Jupp and Kume, 2018] Jupp, P. and Kume, A. (2018). Measures of goodness of fit obtained by canonical transformations on riemannian manifolds. *arXiv preprint arXiv:1811.04866*.
- [Jupp et al., 1979] Jupp, P. E., Mardia, K. V., et al. (1979). Maximum likelihood estimators for the matrix von mises-fisher and bingham distributions. *The Annals of Statistics*, 7(3):599–606.
- [Kanagawa et al., 2019] Kanagawa, H., Jitkrittum, W., Mackey, L., Fukumizu, K., and Gretton, A. (2019). A kernel stein test for comparing latent variable models. *arXiv preprint arXiv:1907.00586*.
- [Kim et al., 2016] Kim, B., Khanna, R., and Koyejo, O. (2016). Examples are not enough, learn to criticize! criticism for interpretability. In *Proceedings of the 30th International Conference on Neural Information Processing Systems*, pages 2288–2296.
- [Klein et al., 2020] Klein, N., Orellana, J., Brincat, S. L., Miller, E. K., Kass, R. E., et al. (2020). Torus graphs for multivariate phase coupling analysis. *Annals of Applied Statistics*, 14(2):635–660.
- [Le et al., 2020] Le, H., Lewis, A., Bharath, K., and Fallaize, C. (2020). A diffusion approach to stein’s method on riemannian manifolds. *arXiv preprint arXiv:2003.11497*.
- [Lee, 1990] Lee, A. J. (1990). *U-Statistics: Theory and Practice*. CRC Press.
- [Lee, 2018] Lee, J. M. (2018). *Introduction to Riemannian manifolds*. Springer.
- [Ley et al., 2017] Ley, C., Reinert, G., Swan, Y., et al. (2017). Stein’s method for comparison of univariate distributions. *Probability Surveys*, 14:1–52.
- [Ley and Verdebout, 2017] Ley, C. and Verdebout, T. (2017). *Modern directional statistics*. Chapman and Hall/CRC.
- [Liu and Zhu, 2018] Liu, C. and Zhu, J. (2018). Riemannian stein variational gradient descent for bayesian inference. In *Thirty-Second AAAI Conference on Artificial Intelligence*.
- [Liu et al., 2016] Liu, Q., Lee, J., and Jordan, M. (2016). A kernelized stein discrepancy for goodness-of-fit tests. In *International Conference on Machine Learning*, pages 276–284.

- [Liu and Kanamori, 2019] Liu, S. and Kanamori, T. (2019). Estimating density models with complex truncation boundaries. *arXiv preprint arXiv:1910.03834*.
- [Lloyd and Ghahramani, 2015] Lloyd, J. R. and Ghahramani, Z. (2015). Statistical model criticism using kernel two sample tests. *Advances in Neural Information Processing Systems*, 28:829–837.
- [Ma et al., 2015] Ma, Y.-A., Chen, T., and Fox, E. (2015). A complete recipe for stochastic gradient mcmc. In *Advances in Neural Information Processing Systems*, pages 2917–2925.
- [Mardia and Jupp, 1999] Mardia, K. V. and Jupp, P. E. (1999). *Directional Statistics*. Wiley, New York, NY.
- [Mardia et al., 2016] Mardia, K. V., Kent, J., and Laha, A. (2016). Score matching estimators for directional distributions. *arXiv:1604.08470*.
- [Muandet et al., 2017] Muandet, K., Fukumizu, K., Sriperumbudur, B., Schölkopf, B., et al. (2017). Kernel mean embedding of distributions: A review and beyond. *Foundations and Trends® in Machine Learning*, 10(1-2):1–141.
- [Pawlowsky-Glahn and Buccianti, 2011] Pawlowsky-Glahn, V. and Buccianti, A. (2011). *Compositional data analysis: Theory and applications*. John Wiley & Sons.
- [Pourzanjani et al., 2017] Pourzanjani, A. A., Jiang, R. M., Mitchell, B., Atzberger, P. J., and Petzold, L. R. (2017). General bayesian inference over the stiefel manifold via the givens representation. *arXiv preprint arXiv:1710.09443*.
- [Sei et al., 2013] Sei, T., Shibata, H., Takemura, A., Ohara, K., and Takayama, N. (2013). Properties and applications of fisher distribution on the rotation group. *Journal of Multivariate Analysis*, 116:440–455.
- [Serfling, 2009] Serfling, R. J. (2009). *Approximation theorems of mathematical statistics*, volume 162. John Wiley & Sons.
- [Seth et al., 2019] Seth, S., Murray, I., Williams, C. K., et al. (2019). Model criticism in latent space. *Bayesian Analysis*, 14(3):703–725.
- [Singh et al., 2002] Singh, H., Hnizdo, V., and Demchuk, E. (2002). Probabilistic model for two dependent circular variables. *Biometrika*, 89:719–723.
- [Song et al., 2009] Song, L., Huang, J., Smola, A., and Fukumizu, K. (2009). Hilbert space embeddings of conditional distributions with applications to dynamical systems. In *Proceedings of the 26th Annual International Conference on Machine Learning*, pages 961–968.
- [Spivak, 2018] Spivak, M. (2018). *Calculus on manifolds: a modern approach to classical theorems of advanced calculus*. CRC press.

- [Sriperumbudur et al., 2011] Sriperumbudur, B. K., Fukumizu, K., and Lanckriet, G. R. (2011). Universality, characteristic kernels and rkhs embedding of measures. *Journal of Machine Learning Research*, 12(Jul):2389–2410.
- [Sutherland et al., 2016] Sutherland, D. J., Tung, H.-Y., Strathmann, H., De, S., Ramdas, A., Smola, A., and Gretton, A. (2016). Generative models and model criticism via optimized maximum mean discrepancy. *arXiv preprint arXiv:1611.04488*.
- [Uehara et al., 2020] Uehara, M., Matsuda, T., and Kim, J. K. (2020). Imputation estimators for unnormalized models with missing data. In *International Conference on Artificial Intelligence and Statistics*, pages 831–841. PMLR.
- [Van der Vaart, 2000] Van der Vaart, A. W. (2000). *Asymptotic statistics*, volume 3. Cambridge university press.
- [Xu and Matsuda, 2020] Xu, W. and Matsuda, T. (2020). A stein goodness-of-fit test for directional distributions. In *International Conference on Artificial Intelligence and Statistics*, pages 831–841. PMLR.
- [Yang et al., 2018] Yang, J., Liu, Q., Rao, V., and Neville, J. (2018). Goodness-of-fit testing for discrete distributions via stein discrepancy. In *International Conference on Machine Learning*, pages 5557–5566.
- [Yang et al., 2019] Yang, J., Rao, V., and Neville, J. (2019). A stein–papangelou goodness-of-fit test for point processes. In *The 22nd International Conference on Artificial Intelligence and Statistics*, pages 226–235.

Supplementary Material for Interpretable Stein Goodness-of-fit Tests on Riemannian Manifolds

A Proofs and Derivations

Stein's Identity

Proof of Theorem 1

Proof. Let $\omega = \sum_{i=1}^d f^i d\theta^{(-i)}$, where

$$d\theta^{(-i)} = d\theta^{i+1} \wedge \dots \wedge d\theta^d \wedge d\theta^1 \dots \wedge d\theta^{i-1}$$

for $i = 1, \dots, d$. Then,

$$d(qJ\omega) = \sum_{i=1}^d \left(\frac{\partial f^i}{\partial \theta^i} + f^i \frac{\partial}{\partial \theta^i} \log(qJ) \right) d\theta^1 \wedge \dots \wedge d\theta^d = (qJ\mathcal{A}_q^{(1)}\mathbf{f})d\theta^1 \wedge \dots \wedge d\theta^d.$$

Therefore, from Theorem 1 and Corollary 1,

$$\mathbb{E}_q[\mathcal{A}_q^{(1)}\mathbf{f}] = \int_{\mathcal{M}} d(qJ\omega) = 0.$$

□

Quadratic form of mKSD

Proof of Theorem 2

Proof. We show that, the mKSD admits the form of taking expectation over p for bivariate functions $h_q^{(c)}$ which is independent of p . $h_q^{(c)}$ is also referred as the Stein kernel. The proof utilize the reproducing property of relevant RKHS and the fact that $\mathcal{A}_q^{(c)}$ is a linear functional of relevant test function f .

For $c = 1$, the test function is a stack of d -dimensional RKHS functions $\mathbf{f} \in \mathcal{H}^d$. $\mathbb{E}_p[\mathcal{A}_q^{(1)}\mathbf{f}]$ is a linear functional of $\mathbf{f} \in \mathcal{H}^d$. Then, from the Riesz representation theorem, there uniquely exists $\mathbf{r} = (r_1, \dots, r_d) \in \mathcal{H}^d$ such that $\mathbb{E}_p[\mathcal{A}_q^{(1)}\mathbf{f}] = \langle \mathbf{f}, \mathbf{r} \rangle_{\mathcal{H}^d}$. By using the reproducing property of \mathcal{H} associate with kernel k , we obtain

$$r_i(x) = \mathbb{E}_{\tilde{x} \sim p} \left[k(x, \tilde{x}) \frac{\partial}{\partial \tilde{\theta}^i} \log(qJ) + \frac{\partial}{\partial \tilde{\theta}^i} k(x, \tilde{x}) \right], \quad (17)$$

for $i = 1, \dots, d$. Thus, the maximization in $\text{mKSD}^{(1)}(p||q)$ is attained by $\mathbf{f} = \mathbf{r}/\|\mathbf{r}\|_{\mathcal{H}^d}$ and $\text{mKSD}^{(1)}(p||q)^2 = \|\mathbf{r}\|_{\mathcal{H}^d}^2$. Therefore, the quadratic form is obtained after

straightforward calculations:

$$\begin{aligned} \text{mKSD}^{(1)}(p||q)^2 &= \left\langle \mathbb{E}_{x \sim p}[\mathcal{A}_q^{(1)}k(x, \cdot)], \mathbb{E}_{\tilde{x} \sim p}[\mathcal{A}_q^{(1)}k(\tilde{x}, \cdot)] \right\rangle_{\mathcal{H}^d} \\ &= \mathbb{E}_{x, \tilde{x} \sim p} \left[\underbrace{\left\langle \mathcal{A}_q^{(1)}k(x, \cdot), \mathcal{A}_q^{(1)}k(\tilde{x}, \cdot) \right\rangle_{\mathcal{H}^d}}_{h_q^{(1)}(x, \tilde{x})} \right], \end{aligned}$$

and the assertion follows.

For $c = 2$, similar argument applies where the test function is a scalar-valued RKHS $\tilde{f} \in \mathcal{H}$. Instead of Eq.(17), we have $\tilde{r} \in \mathcal{H}$, s.t. $\mathbb{E}_p[\mathcal{A}_q^{(2)}\mathbf{f}] = \langle \tilde{f}, \tilde{r} \rangle_{\mathcal{H}}$ and

$$\tilde{r}(x) = \mathbb{E}_{\tilde{x} \sim p} \left[\sum_{ij} g^{ij} \left(\frac{\partial}{\partial \tilde{\theta}^j} k(x, \tilde{x}) \frac{\partial}{\partial \theta^i} \log(qJ) + \frac{\partial^2}{\partial \tilde{\theta}^i \partial \tilde{\theta}^j} k(x, \tilde{x}) \right) \right], \quad (18)$$

and the maximization in $\text{mKSD}^{(2)}(p||q)$ is attained by $\tilde{f} = \tilde{r}/\|\tilde{r}\|_{\mathcal{H}}$; thus $\text{mKSD}^{(2)}(p||q)^2 = \|\tilde{r}\|_{\mathcal{H}}^2$. The assertion then follows from the similar calculations as above.

For $c = 0$, the quadratic form is readily obtained from derivation of maximum-mean-discrepancy (MMD) [Gretton et al., 2007] form as shown in Theorem 4. Alternatively, for scalar test function $h \in \mathcal{H}$, we can write,

$$\text{mKSD}^{(0)}(p||q) = \sup_{\|h\|_{\mathcal{H}} \leq 1} \mathbb{E}_p[\mathcal{A}_q^{(0)}h] = \sup_{\|h\|_{\mathcal{H}} \leq 1} |\mathbb{E}_p[h] - \mathbb{E}_q[h]|,$$

where taking the supreme we get,

$$\begin{aligned} \text{mKSD}^{(0)}(p||q)^2 &= \left\langle \mathbb{E}_p[k(x, \cdot) - \mathbb{E}_q[k(x, \cdot)]], \mathbb{E}_p[k(\tilde{x}, \cdot) - \mathbb{E}_q[k(\tilde{x}, \cdot)]] \right\rangle_{\mathcal{H}} \\ &= \mathbb{E}_{x, \tilde{x} \sim p} \left\langle \underbrace{k(x, \cdot) - \mathbb{E}_q[k(x, \cdot)]}_{\mathcal{A}_q^{(0)}k(x, \cdot)}, k(\tilde{x}, \cdot) - \mathbb{E}_q[k(\tilde{x}, \cdot)] \right\rangle_{\mathcal{H}}. \end{aligned}$$

The assertion follows. \square

The quadratic form is useful when computing the empirical estimate for the expectation where only samples from unknown distribution p is observed. We also note that $\mathbb{E}_q[k(\tilde{x}, \cdot)]$, in general, is not possible to obtain in analytical form, especially when the density q is only given up to normalization. Samples from q , if possible to obtain from unnormalized density, can be useful to estimate $\mathcal{A}_q^{(0)}k(x, \cdot)$, where we denote as $\widehat{\mathcal{A}_q^{(0)}}k(x, \cdot)$.

Characterisation of mKSD

Proof of Theorem 3

Proof. Denote $\mathbf{s}_p^{(c)}(\cdot) = \mathbb{E}_{\tilde{x} \sim p}[\mathcal{A}_q^{(c)}k(\tilde{x}, \cdot)] \in \mathcal{F}$ and we can write

$$\text{mKSD}^{(c)}(p\|q)^2 = \|\mathbf{s}_p(\cdot)\|_{\mathcal{F}}^2 \geq 0,$$

where \mathcal{F} can be \mathcal{H} for $c = 0, 2$ or \mathcal{H}^d for $c = 1$. If $p = q$, then $\text{mKSD}^{(c)}(p\|q)^2 = 0$ from the Stein identity.

Conversely, if $\text{mKSD}^{(c)}(p\|q)^2 = 0$, then $\mathbf{s}_p^{(c)}(x) = \mathbf{0}$, a zero vector in \mathbb{R}^d for $c = 1$ and a scalar zero in \mathbb{R} for $c = 0, 2$, $\forall x$, s.t. $p(x) > 0$. Then, from $\log(q/p) = \log(qJ) - \log(pJ)$, we obtain,

$$\mathbb{E}_{\tilde{x} \sim p} [L_i(\tilde{x})k(\tilde{x}, x)] = (\mathbf{s}_p^{(1)})_i(x) - \mathbb{E}_{\tilde{x} \sim p} [\mathcal{A}_p^{(1)}k(\tilde{x}, x)] = 0,$$

and

$$\mathbb{E}_{\tilde{x} \sim p} [L(\tilde{x})k(\tilde{x}, x)] = (\mathbf{s}_p^{(c)})(x) - \mathbb{E}_{\tilde{x} \sim p} [\mathcal{A}_p^{(c)}k(\tilde{x}, x)] = 0,$$

for $c = 0, 2$, for every x with positive densities. Since k is compact-universal, vanishes at $\partial\mathcal{M}$ and \mathcal{M} is smooth and compact, the injectivity result in [Carmeli et al., 2010, Theorem 4(b)] implies that $L_i^{(1)} = 0, \forall i$ (for $c = 1, i \in \{1, \dots, d\}$; for $c = 0, 2, i = 1$). Therefore, $\log(q/p)$ is constant on \mathcal{M} . Since both p and q are both densities on \mathcal{M} that integrate to one, we conclude $p = q$. \square

Asymptotics of mKSD

Proof of Theorem 5

Proof. To show part 1, it is enough to check the mKSD statistics is degenerate U-statistics under $H_0 : p = q$. By considering test function $f = k(x, \cdot)$ (or its relevant vector-valued form for $c = 1$), Stein identity shows that,

$$\mathbb{E}_{\tilde{x} \sim p}[\mathcal{A}_q^{(c)}k(x, \tilde{x})] = 0, \forall x \in \mathcal{M},$$

so that the variance $\sigma_c^2 = 0$ for $c = 0, 1, 2$. Then the standard results for degenerate U-statistics in [Serfling, 2009, Section 5.5.2] apply and the assertions follow.

In addition, it is interesting to note link the result for $c = 0$ with the asymptotic result in as

$$h_q^{(0)}(x, \tilde{x}) = k(x, \tilde{x}) - \xi(x) - \xi(\tilde{x}) + C,$$

where $C = \mathbb{E}_{x, \tilde{x} \sim q}k(x, \tilde{x})$ is a constant, $\xi(x) = \mathbb{E}_{\tilde{x} \sim q}k(x, \tilde{x})$ is only a function of x and $\xi(\tilde{x}) = \mathbb{E}_{x \sim q}k(x, \tilde{x})$ is only a function of \tilde{x} . The formulation is analogous to the asymptotic results for MMD, as shown in [Gretton et al., 2007, Theorem 8]: $h_q^{(0)}(x, \tilde{x})$ is equivalent to the notion of $\tilde{k}(x, \tilde{x})$ in [Gretton et al., 2007].

Part 2 follows as $\sigma_c^2 > 0$ under $H_1 : p \neq q$ by Theorem 3. Apply asymptotic distribution of non-degenerate U-statistics [Serfling, 2009, Section 5.5.1] and the assertions follow. \square

Asymptotics for mFSSD To compute the empirical version of mFSSD, we consider the empirical version $\mathbf{s}_p(\cdot)$ in Eq.(15) from samples $x_1, \dots, x_n \sim p$:

$$\widehat{\mathbf{s}}_p(\cdot) = \frac{1}{n} \sum_i [\mathcal{A}_q^{(1)} k(x_i, \cdot)].$$

Then the empirical mFSSD has the form

$$\widehat{\text{mFSSD}}^2 = \frac{1}{dJ} \sum_{i=1}^d \sum_{j=1}^J (\widehat{\mathbf{s}}_p(\mathbf{v}_j))_i^2, \quad (19)$$

for any set of test locations $\{\mathbf{v}_j\}_{j=1}^J$.

Proposition 3. *Assume the conditions in Theorem 3 hold, and $\mathbb{E}_{x \sim p}[\|\mathbf{s}_p(x)\|^2] < \infty$. Under $H_1 : p \neq q$,*

$$\sqrt{n} \cdot \left(\widehat{\text{mFSSD}}^2 - \text{mFSSD}^2 \right) \xrightarrow{d} \mathcal{N}(0, \tilde{\sigma}_{H_1}^2),$$

where $\tilde{\sigma}_{H_1}^2$ denotes the variance for $\widehat{\text{mFSSD}}^2$.

Proof. With the assumed regularity conditions, Eq.(19) is in the form of the non-degenerate U-statistics with $\tilde{\sigma}_{H_1}^2 > 0$. The asymptotic normality follows from [Serfling, 2009, Section 5.5.1], similarly described in [Jitkrittum et al., 2017, Proposition 2]. \square

The asymptotic normality for $\widehat{\text{mFSSD}}^2$ in Proposition 3 enables derivation of the approximate test power, similarly as described in Section 4.2 for kernel choice.

Proposition 4. [Approximate test power of $n \cdot \widehat{\text{mFSSD}}^2$] *Under H_1 , for large n and fixed r , the test power is*

$$\mathbb{P}_{H_1}(n \cdot \widehat{\text{mFSSD}}^2 > r) \approx 1 - \Phi \left(\frac{r}{\sqrt{n} \tilde{\sigma}_{H_1}^2} - \sqrt{n} \frac{\text{mFSSD}^2}{\tilde{\sigma}_{H_1}^2} \right),$$

where Φ denotes the cumulative distribution function of the standard normal distribution, and $\tilde{\sigma}_{H_1}^2$ is defined in Proposition 3.

Due to \sqrt{n} scaling in Proposition 3, maximizing the approximate test power for $n \cdot \widehat{\text{mFSSD}}^2$ can be approximated by maximizing $\frac{\text{mFSSD}^2}{\tilde{\sigma}_{H_1}^2}$ to obtain optimal test locations under the alternative $H_1 : p \neq q$, which is described in Section 5.

$$V = \arg \max_{\mathbf{v}} \frac{\text{mFSSD}^2}{\tilde{\sigma}_{H_1}^2},$$

for $V = \{\mathbf{v}_j\}_{j=1}^J$ as the set of test locations to be optimised.

B More on Bahadur Efficiency

In this section, we introduce the relevant concepts to study Approximate Relative Efficiency (ARE) between two tests, characterised by *Bahadur slope* [Bahadur et al., 1960] and corresponding *Bahadur efficiency*.

B.1 Approximate Bahadur Slope

We first define Bahadur slope for general tests [Gleser, 1966] and its applications in kernel-based tests [Jitkrittum et al., 2017, Garreau et al., 2017]. Consider the test procedure with null hypothesis $H_0 : \omega \in \Omega_0$ and the alternative $H_1 : \omega \in \Omega \setminus \Omega_0$, where Ω and Ω_0 are arbitrary sets. Denote T_n as the test statistic computed from a sample of size n .

Definition 1. For $\omega_0 \in \Omega_0$, let F be the asymptotic null distribution

$$F(t) = \lim_{n \rightarrow \infty} \mathbb{P}_{\omega_0}(T_n < t)$$

which is assumed to be continuous and common $\forall \omega_0 \in \Omega_0$. Assume that there exists a continuous strictly increasing function $\rho : (0, \infty) \rightarrow (0, \infty)$ s.t $\lim_{n \rightarrow \infty} \rho(n) = \infty$. Denote

$$c(\omega) = -2 \text{plim}_{n \rightarrow \infty} \frac{\log(1 - F(T_n))}{\rho(n)}, \quad (20)$$

for some bounded non-negative function c such that $c(\omega_0) = 0$ when $\omega_0 \in \Omega_0$. The function $c(\omega)$ is known as approximate Bahadur slope.

Definition 2. Let $\mathcal{D}(a, t)$ be a class of all continuous cumulative distribution functions (CDF) F such that $-2 \log(1 - F(x)) = ax^t(1 + o(1))$, as $x \rightarrow \infty$ for $a > 0$ and $t > 0$.

Proposition 5. The approximate Bahadur slope (ABS) for the tests with $\text{mKSD}^{(c)}$, $c = 0, 1, 2$ is

$$c^{(\text{mKSD}^{(c)})} := \frac{\mathbb{E}_p[h_q^{(c)}(x, \tilde{x})]}{\mathbb{E}_q[h_q^{(c)}(x, \tilde{x})^2]^{\frac{1}{2}}},$$

where $h_q^{(c)}(x, \tilde{x})$ is the Stein kernel for $\text{mKSD}^{(c)}$, and $\rho(n) = n$.

Proof. Using Theorem 9 and Theorem 11 in [Jitkrittum et al., 2017], we know that $n \cdot \text{mKSD}_u^{(c)}(p||q)^2$ in Eq.(9) is in the class of $\mathcal{D}(a = 1/\omega_c, t = 1)$ for ω_c^2 is the variance of the statistic. By Stein identity, $\mathbb{E}_{x \sim q} \mathbb{E}_{\tilde{x} \sim q} [h_q^{(c)}(x, \tilde{x})]^2 = 0$. Hence, using second point in Theorem 9 [Jitkrittum et al., 2017] and choosing $\rho = n$, we know that $n \cdot \text{mKSD}_u^{(c)}(p||q)^2 \setminus \rho(n) \rightarrow \text{mKSD}^{(c)}(p||q)^2$ by weak law of large numbers. \square

B.2 Asymptotic Relative Efficiencies Between mKSD Tests with Different \mathcal{A}_q s

Asymptotic Relative Efficiency (ARE) between two statistical testing procedures measures how fast the p-values of one test shrinks to 0, relatively to the other's. If it is faster, for given problem under the alternative, it is more sensitive to pick up the alternative, where we call the test more "statistically efficient". With ABS, we are ready to define approximate Bahadur efficiency.

Definition 3. Given two sequences of test statistics, $T_n^{(1)}$ and $T_n^{(2)}$ and their ABS $c^{(1)}$ and $c^{(2)}$, the approximate Bahadur efficiency of $T_n^{(1)}$ relative to $T_n^{(2)}$ is

$$E(\omega_A) := \frac{c^{(1)}(\omega_A)}{c^{(2)}(\omega_A)} \quad (21)$$

for $\omega_A \in \Omega \setminus \Omega_0$, in the space of alternative models.

If $E(\omega_A) > 1$, then $T_n^{(1)}$ is asymptotically more efficient than $T_n^{(2)}$ in the sense of Bahadur, for the particular problem specified by $\omega_A \in \Omega \setminus \Omega_0$.

B.3 The Case Study on Circular distribution \mathcal{S}^1

Proof of Theorem 6

Proof. To compute $E_{1,2}(\kappa)$, we can rewrite the following:

$$E_{1,2}(\kappa) = \frac{\mathbb{E}_p[h_q^{(1)}(x, \tilde{x})]}{\mathbb{E}_p[h_q^{(2)}(x, \tilde{x})]} \cdot \frac{\mathbb{E}_q[h_q^{(2)}(x, \tilde{x})^2]^{\frac{1}{2}}}{\mathbb{E}_q[h_q^{(1)}(x, \tilde{x})^2]^{\frac{1}{2}}}$$

The second term only involves integrals over $q(x) \propto 1$, which is independent of κ and we can solve it as $\frac{\mathbb{E}_q[h_q^{(2)}(x, \tilde{x})^2]^{\frac{1}{2}}}{\mathbb{E}_q[h_q^{(1)}(x, \tilde{x})^2]^{\frac{1}{2}}} = 1.692 > 1$. For the first term, the ratio is monotonic decreasing w.r.t. $\kappa > 0$ and $\frac{\mathbb{E}_p[h_q^{(1)}(x, \tilde{x})]}{\mathbb{E}_p[h_q^{(2)}(x, \tilde{x})]}$ is lower bounded by 2 due to exponential-trace kernel and \mathcal{S}^1 embedded in \mathbb{R}^2 . Hence, for $\kappa > 0$, $E_{1,2} > 1$. \square

We can apply similar approach to compare the relative test efficiency $E_{0,1}(\kappa)$ between $\text{mKSD}^{(0)}$ and $\text{mKSD}^{(1)}$. We plot numerical solutions in Figure 3. From Figure 3, we see that $E_{1,2}$ and $E_{0,1}$ both greater than 1 for $\kappa \in (0, 20)$. For further increase of κ , there is a trend for both relative efficiencies stabilizing at some value greater than 1. Theoretical analysis for such limiting behaviour is of an interesting future topic.

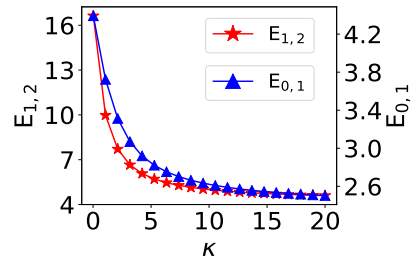


Figure 3: Relative Test Efficiency

Although Figure 3 shows that $\mathbb{E}_{0,1}(\kappa) > 1$ for small perturbation from the null, i.e. $\kappa \in (0, 20)$ which suggest the relative efficiency of $\text{mKSD}^{(0)}$ is higher than the first order test $\text{mKSD}^{(1)}$, it is usually not possible to compute MMD analytically and the normalized density is required.

Intuitively, with sampling error of order \sqrt{n} and $\rho(n) = n$ is chosen to compute Bahadur slope, the MMD computed from samples are less efficient to perform goodness-of-fit test compared to mKSD tests that directly access the unnormalized density, as shown in Figure 1. Similar findings are also observed in other settings where MMD is considered to perform goodness-of-fit tests [Liu et al., 2016, Jitkritum et al., 2017, Yang et al., 2018, Yang et al., 2019, Xu and Matsuda, 2020]. In addition, correctly sampling from Riemannian manifold is non-trivial and can be time-consuming for sample-based tests.

C More on Model Criticism

In this section, we provide additional details on model criticism for wind data present in Section 8.2. We fitted the model in Eq.(2) by using noise contrastive estimation [Uehara et al., 2020] and our test does not find evidence to reject the fitted model, suggesting a good fit for the wind direction data. In addition, we consider the model without interaction term between two directions:

$$\tilde{q}(x_1, x_2 | \tilde{\xi}) \propto \exp\{\kappa_1 \cos(x_1 - \mu_1) + \kappa_2 \cos(x_2 - \mu_2)\}, \quad (22)$$

which is equivalent to model in Eq.(2) by imposing $\lambda_{12} = 0$. This model can be viewed as product of marginal distributions of x_1 and x_2 and we refer as factorized model. Our test reject the null at test level $\alpha = 0.05$ suggesting a poor fit of the factorized model.

To further visualize the difference between models in Eq.(2) and Eq.(22), we plot histogram of each wind direction in Figure 4(b) and samples from the factorized model \tilde{q} in Figure 4(c) where no interactions are present between x_1 and x_2 . Compare with the wind direction data, shown again in Figure 4(a), we can see that Figure 4(c) differs the most at the regions of $\tilde{x} = (x_1, x_2) = (2.8, \pi)$ (data model denser) and $\tilde{x}' = (x_1, x_2) = (1, 1)$ (\tilde{q} model denser). Such difference is captured by our optimized test locations from mFSSD in Figure 4(e), where \tilde{x} is at the region with 3 stars in a row and \tilde{x}' is around the region with 4-stars in a row. It shows the effectiveness of mFSSD in distinguishing the differences between distributions. As \tilde{q} is referred as imposing data model in Eq.(2) to be 0, a negative $\lambda_{12} = -1.1274 < 0$ in the data model implies that positive $\sin(x_1 - \mu_1) \sin(x_2 - \mu_2)$ is less dense. With $\mu_1 = 1.1499 = \mu_2$, $\sin(x_1 - \mu_1) \sin(x_2 - \mu_2)$ is positive around the region the \tilde{x}' making the data model less dense, as shown in Figure 4(a) and 4(c).

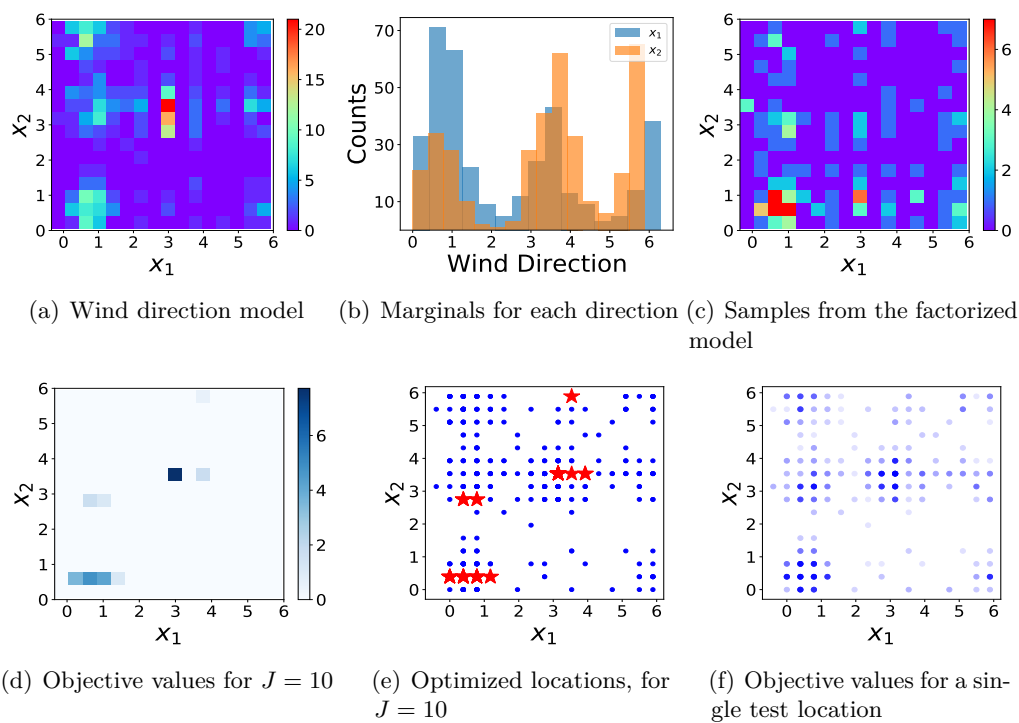


Figure 4: Visualizing the fitted model and rejected model for wind direction data.